

Title	Effect of Heat Cycle in Multi-layer Welding on Charpy Absorbed Energy in Low and High Toughness Steel
Author(s)	Sakino, Yoshihiro; Kim, You-Chul
Citation	Transactions of JWRI. 40(2) P.69-P.75
Issue Date	2011-12
Text Version	publisher
URL	<a href="http://hdl.handle.net/11094/10763">http://hdl.handle.net/11094/10763</a>
DOI	
rights	

***Osaka University Knowledge Archive : OUKA***

<https://ir.library.osaka-u.ac.jp/repo/ouka/all/>

## Effect of Heat Cycle in Multi-layer Welding on Charpy Absorbed Energy in Low and High Toughness Steel

SAKINO Yoshihiro\* and KIM You-Chul\*\*

### Abstract

*In this study, the heat cycle is determined in the case of multi-layer welding using three-dimensional heat-conduction analysis. The relationship between the heat cycle of multi-layer welding and the absorbed energy is defined by simulating various heat cycles of multi-layer welding by performing the synthetic HAZ test using steel with a relatively high Charpy absorbed energy and steel with a relatively low Charpy absorbed energy. On the basis of this relationship, the authors have studied the effects of heat cycle conditions on the Charpy absorbed energy of weld interfaces. In the results, the Charpy absorbed energy increased more than in the case of single-pass welding in some heat cycle in the case of multi-layer welding, both in high-toughness steel and low-toughness steel. The Charpy absorbed energy of the weld interface was greatly susceptible to the achieved temperature after the maximum achieved temperature, and the range of the temperature after the maximum temperature was achieved in which the Charpy absorbed energy was found to be different depending on the steel toughness.*

**KEY WORDS:**(Welding heat affected zone) (Synthetic heat-affected zone test) (Charpy absorbed energy) (Multi-layer welding) (Heat-conduction analysis)

### 1. Introduction

Extensive study of the required toughness of base materials and weld metals has been conducted through full-scale and model experiments in order to prevent brittle fractures of beam-to-column connections and improve their deformation capacities. Heat-affected zones (HAZs) formed as a result of welding where toughness may be very low are also attracting attention, and research has been conducted on specimens that have been cut out from actual HAZs. At present, the Charpy absorbed energy is widely adopted as a factor that can be controlled to prevent brittle fractures. The Charpy absorbed energy at 0 °C of 27 J and 47 J, which are required for steel and weld metals in order to prevent low-stress brittle fractures, and 70 J, (which is proposed as the value required for preventing general yield brittle fractures), have been used in Japan. However, unlike base materials and weld metals, in HAZs, large changes in the material properties are observed in a small area. Therefore, the toughness test methods, such as the crack tip opening displacement (CTOD) test and the Charpy impact test often fail to produce accurate results because

of factors such as the displacement of the notch tip from the desired position and the progress of cracks outside the area of analysis. As described above, it is difficult to determine the local toughness of HAZs using actual welding materials. A potential solution could be to adopt a synthetic HAZ test for estimating toughness in which HAZs are simulated using a simulated thermal-cycle device. The simulated thermal cycle device can simulate various heat processes using rapid high-temperature heating by applying an electrical current, and it can simulate the welded material after recrystallization as homogeneous materials. When a homogeneous material is used, variations resulting from heterogeneity of material properties can be eliminated, and local portions to be analyzed can be tested precisely using various evaluation tests such as the CTOD test and the Charpy impact test. The synthetic HAZ test was also used to test the strength properties, which are as important as the Charpy impact properties in characterizing HAZs, to examine the relationship between the strain required for initiating ductile cracks and the material properties<sup>1)</sup>, and to determine the tensile strength at high-speed loading<sup>2)</sup>.

The authors focused on 400-MPa-grade and 490-MPa-grade structural steels as test materials, and

† Received on December 26, 2011

\* Assistant Professor

\*\* Professor

Transactions of JWRI is published by Joining and Welding Research Institute, Osaka University, Ibaraki, Osaka 567-0047, Japan

## Effect of Heat Cycle in Multi-layer Welding on Charpy Absorbed Energy

**Table 1** Tensile test results and chemical composition

	Tensile test results				Chemical composition (mass%)											
	$\sigma_Y$	$\sigma_U$	$\epsilon$	YR	C	Si	Mn	P	S	Cu	Ni	Cr	V	Mo	N	Ceq
	(MPa)	(MPa)	(%)	(%)	$\times 10^{-2}$			$\times 10^{-3}$		$\times 10^{-2}$					$\times 10^{-3}$	$\times 10^{-2}$
High-toughness steel	279	427	34	65	13	21	91	13	4	1	3	1	0	1	0	30
Low-toughness steel	281	456	31	62	24	1	39	20	3	2	2	3	0	1	9	32

$$C_{eq} = C + Si/24 + Mn/6 + Ni/40 + Cr/5 + Mo/4 + V/14$$

simulated CGHAZs, whose toughness is often the lowest among all HAZs, as homogeneous material by the synthetic HAZ test. These CGHAZs were used in the Charpy impact test to determine the Charpy absorbed energy. This enabled the demonstration of the relationship between the equivalent welding-heat input obtained from the cooling time according to the simulated heat cycle and the Charpy absorbed energy. It also allowed their comparison with various standard values, and facilitated a comprehension of the limit values for welding-heat input when the CGHAZs exist as a homogeneous material<sup>3)</sup>. The authors also examined the effects of pre-strain and aging on Charpy absorbed energy at CGHAZs<sup>4)</sup>. However, single-pass welding has been the focus of this study for a considerable period.

In this study, the heat cycle is determined in the case of multi-layer welding using three-dimensional heat-conduction analysis. The relationship between the heat cycle of multi-layer welding and the absorbed energy is defined by simulating various heat cycle of multi-layer welding by performing the synthetic HAZ test using steel with a relatively high Charpy absorbed energy (hereinafter referred to as high-toughness steel) and steel with a relatively low Charpy absorbed energy (hereinafter referred to as low-toughness steel)<sup>5)</sup>. On the basis of this relationship, the authors have studied the effects of heat cycle conditions on the Charpy absorbed energy of weld interfaces of two types of structural steels with different levels of toughness, in the case of

multi-layer welding.

### 2. Outline of experiment

In the experiment, SN400 (rolled steels for building structure, 400-MPa-grade) flat steel (PL-22) was used as the high-toughness steel, and SS400 (rolled steels for general structure, 400-MPa-grade) H section steel (RH-612×202×13×23) was used as the low-toughness steel. **Table 1** shows the tensile test results and chemical composition analysis results of the sample steels in the inspection certificate.

**Figures 1** and **2** show the transition curves obtained by performing the Charpy impact test on the sample steels. The absorbed energy at 0 °C of the high-toughness steel used in this study is about 185 J, which is not a significantly large value. However, since it is considerably larger than the values of 27 to 70 J, standardized or proposed in JIS and in the literature proposed by the Building Center of Japan, this steel is called high-toughness steel in this study. The Charpy absorbed energy at 0 °C of the low-toughness steel is very low (about 15 J), and its energy-transition and fracture-transition temperatures are both very high (approximately 70 °C). CTOD tests using a notched three-point bending specimens were also conducted, and the results showed that the limit of the CTOD value at 0 °C,  $\delta_c$ , was very low (0.0444 mm). As described so far, it could be said that the toughness of the sample steel is very low.

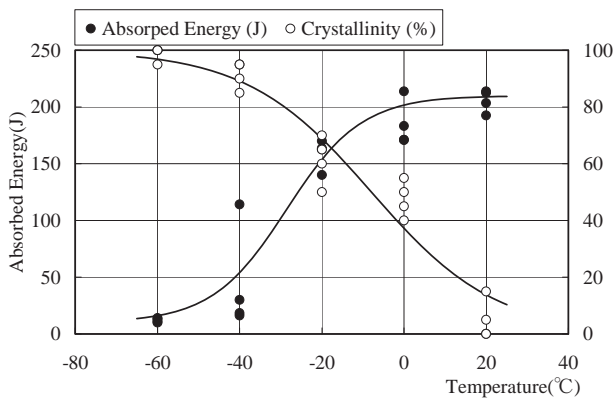


**Fig. 1** Transition curve (high-toughness steel)

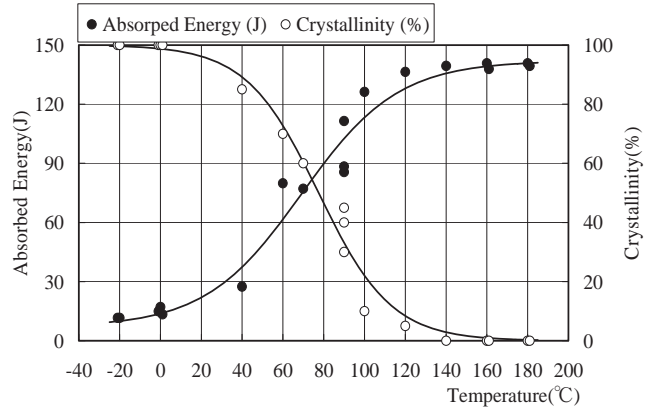


**Fig. 2** Transition curve (low-toughness steel)

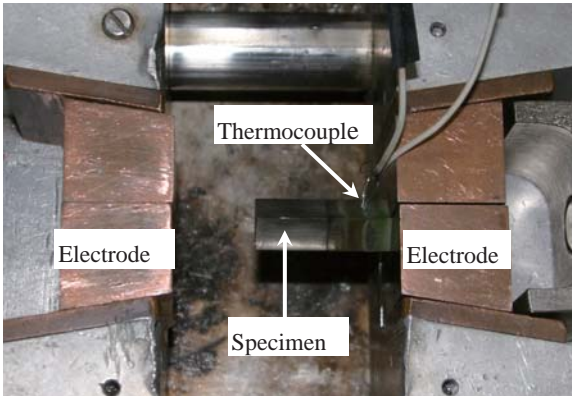


Fig. 3 Synthetic HAZ test

The simulated HAZ specimens of square-rod-shaped (11×11×60 mm) were cut out from the center of the high-toughness steel and the low-toughness steel, and a heat cycle was applied to the central area of these specimens using a simulated thermal cycle device (Gleeble 1500). The temperature was controlled using a Type R thermocouple attached at the center of each specimen, and helium was used as the atmosphere gas. **Figure 3** shows an image of the apparatus after the test. The left-side electrode was moved away from the specimen to allow it to be clearly seen in this image, but was placed in the same manner as the right-side electrode during the test to hold the specimen such that there were 10 mm spaces between both sides of the

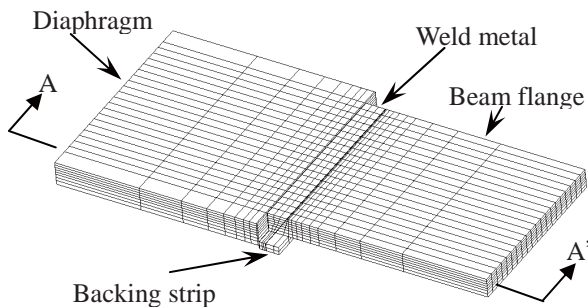


Fig. 4 Analysis model at the butt weld zone between the diaphragm and the beam flange

Table 2 Welding conditions

Pass No.	Current (A)	Voltage (V)	Speed (cm/min)	Interlayer temperature (°C)
1	260	32	34	100
2	260	32	27	160
3	260	32	28	190

electrodes. From the results of the hardness test and from metallographic observation, it was confirmed that the central area to which the heat cycle was applied was a homogeneous material<sup>3)</sup>. After the synthetic HAZ test was performed, the specimens were processed to form full-size V-notched specimens having dimensions of 10×10×55 mm; these V-notched specimens were then used in the Charpy impact test. A Charpy impact tester with a capacity of 490 J was used, and the test temperature was 0 °C. Four pieces of specimen were used for each condition.

When the heat cycle is known, the synthetic HAZ test can simulate the HAZ that was affected by the heat as a homogeneous material, but it is very difficult to determine the heat cycle of an HAZ, especially when it exists inside steel. In such cases, analytical approaches are a possible option to determine the heat cycle. Recent improvements in computing speed and memory also enable heat-conduction analysis of multi-layer welding of a butt weld zone as a full-scale three-dimensional model and as a moving heat source which the welding position continuously changes<sup>6)</sup>.

Then, to determine the welding heat cycle at the weld interface during multi-layer welding, a three-dimensional unsteady-heat-conduction analysis of the butt weld zone between the through diaphragm (PL-23) and the beam (rolled H section steel RH-612×202×13×23 mm) flange was used. **Figure 4** shows an entire mesh drawing; **Figure 5** shows the detailed drawing of the weld zone in the A-A' section (cross

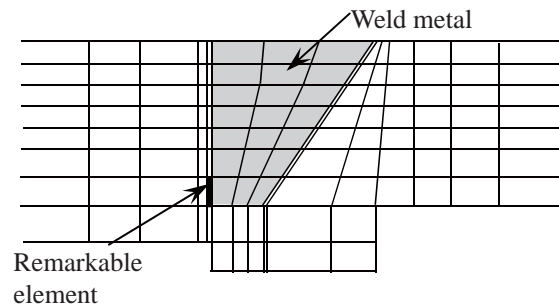


Fig. 5 Detail of the weld zone (A-A' section)

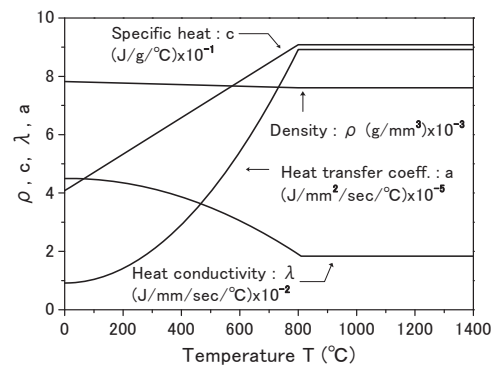
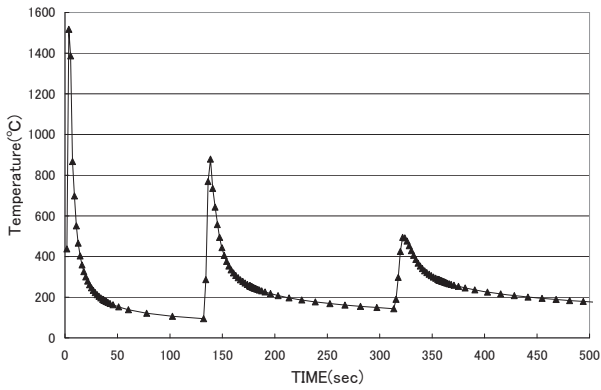


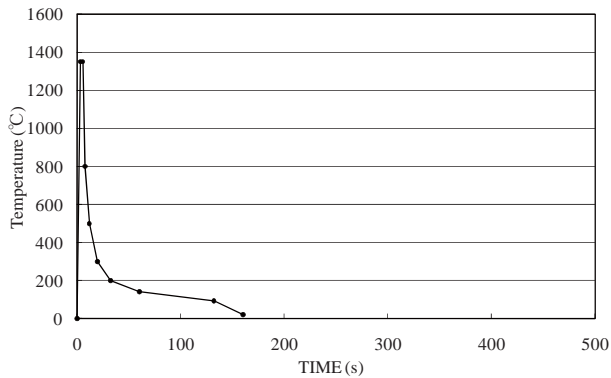
Fig. 6 Temperature dependence of the physical constants<sup>7)</sup>

## Effect of Heat Cycle in Multi-layer Welding on Charpy Absorbed Energy

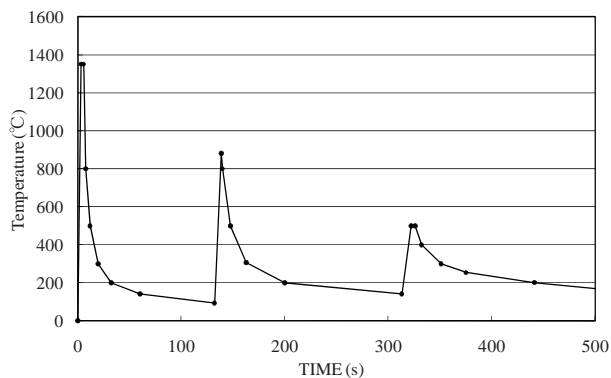


**Fig. 7** Results of three-dimensional heat-conduction analysis

section of the region that is 10 mm inward from the beam end where welding is started). Only the diaphragm (240×240×28 mm), the beam flange (200×250×23 mm), and the backing strip (200×24×9 mm) that were in contact with the weld zone were modeled, and the weld tabs were not considered. The welding is represented as a moving heat source, and heat transfer to the column and beam webs are not taken into consideration. The deposition sequence and the welding conditions conform to the measurement record



(a) Single-run



(b) Multi-layer, High-Intermediate-Low

**Fig. 8** Simulated welding-heat cycle (Comparison between single-pass welding and multi-layer welding)

(Table 2). Figure 6 shows the temperature dependence of the physical constants used in this analysis<sup>7)</sup>. The thermal efficiency is set at 0.8 because the welded area is narrow.

In this study, the heat cycle at the location of an element that is at the weld interface on the first-layer-diaphragm-side of the A-A' section (the black element indicated as "Remarkable element" in Fig. 5) was determined. This section is the origin of the first-layer welding, and it can thus cause weld defects and may become the origin of brittle fracture.

Figure 7 shows the analysis results. The actual welding was for 7 layers and 13 passes, but the figure shows the results up to the third layer and the third pass where the maximum achieved temperature is 500 °C, which is considered as lower limit temperature to influence the structural changes of steels. This study adopts the result shown in Fig. 7, which is obtained from the model shown in Fig. 4, as an example of the heat cycle of the beam-to-column connection, and examines the effects of the heat cycle on the Charpy absorbed energy of the HAZs of two types of steels with different toughness during multi-layer welding.

### 3. Simulated welding heat cycle and experiment results

#### 3.1 Comparison between single-pass welding and multi-layer welding

First, a synthetic HAZ test was conducted using the heat cycle that modeled only the first pass (single-run) and the heat cycle that modeled up to the third layer and the third pass (multi-layer) based on the analysis results. Figures 8(a) and (b) show the heat cycles used for the test.

Figure 9 shows a comparison of the results of the Charpy absorbed energy in the case of the single-pass welding and those in the case of multi-layer welding. This graph shows the values of the Charpy absorbed energy of each specimen (high-toughness steel, H-D

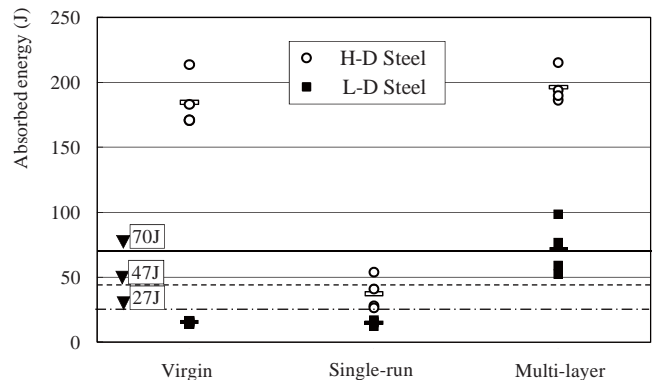


**Fig. 9** Comparison of the Charpy absorbed energies between single-pass welding and multi-layer welding

Steel: ○; low-toughness steel, L-D Steel: ■) and their mean values (H-D Steel: □; L-D Steel: ▣). The figure also shows the standard value for the Charpy absorbed energy, i.e., the standard value 27 J has been represented by a dashed line, the standard value 47 J is represented by a dotted line and the proposed value 70 J is represented by a solid line.

In the case of the high-toughness steel, the Charpy absorbed energy declined significantly in single-pass welding to an average of 47 J or less. However, it increased in multi-layer welding to a level equivalent to that of the base material.

In contrast, in the case of the low-toughness steel, the Charpy absorbed energy remained almost the same in single-pass welding at less than 27 J. However, the Charpy absorbed energy in multi-layer welding increased significantly to approximately 70 J.

Such recovery and increase in the absorbed energy has also been reported in some steel weld zones whose toughness decreased due to cold press bending<sup>8)</sup> or aging<sup>4)</sup>.

As described above, it was found that the Charpy absorbed energy of the weld interface in the case of high-toughness steel decreased significantly to 47 J or below in single-pass welding. Although it increased significantly in multi-layer welding in both the high-toughness and the low-toughness steels, it was

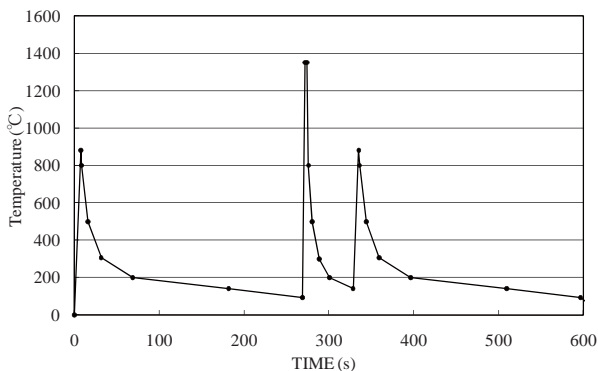
approximately 70 J even in the low-toughness steel.

### 3.2 Effect of the order of maximum achieved temperature

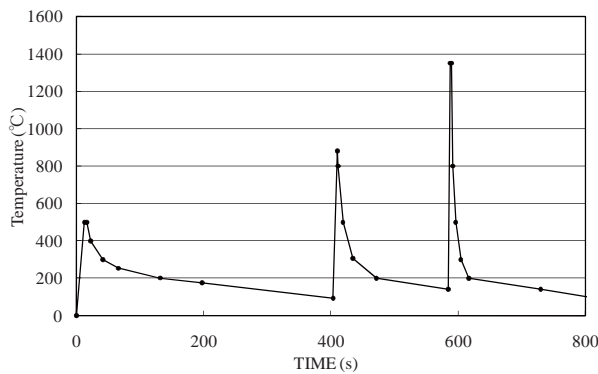
In the weld interface near the middle layer in the case of multi-layer welding, the achieved temperature at each pass increases gradually, and reaches 1350 °C when the nearest layer is welded (when the newest weld is formed) and the achieved temperature then declines in subsequent passes. In the weld interface of the last layer, the achieved temperature at each pass increases gradually as welding progresses, and the maximum achieved temperature reaches 1350 °C when the last layer is welded. In this way, the order of increase and decrease of the achieved temperature differs depending on the position of the weld interface. It is known that the local toughness in multi-layer welding is affected by these maximum temperatures achieved at each pass. Therefore, to study the effect of the order of increase and decrease of the achieved temperature on the Charpy absorbed energy, the synthetic HAZ test was also conducted for the heat cycle of the achieved temperatures in the order of 880–1350–880 °C (Intermediate–High–Intermediate) and 500–880–1350 °C (Low–Intermediate–High). Intermediate–High–Intermediate and Low–Intermediate–High modeled the heat cycle of the weld interface of the middle layer and the last layer, respectively, by rearranging the order of the achieved temperatures of the heat cycle shown in Fig. 8 (b), which modeled the heat cycle of the weld interface near the first layer with the achieved temperatures in the order of 1350–880–500 °C (High–Intermediate–Low). **Figure 10 (a) and (b)** show each heat cycle.

**Figure 11** shows the relationship between the order of increase and decrease of the achieved temperature at each pass and the Charpy absorbed energy.

In the high-toughness steel, the Charpy absorbed energy declined when the order was Intermediate –High –Intermediate, which simulated the HAZ of the middle layer. However, the Charpy absorbed energy was approximately 110 J, which is higher than 70 J. On



(a) Intermediate-High-Intermediate



(b) Low-Intermediate-High

**Fig 10** Simulated welding heat cycle (Effect of the order of achieved temperatures)

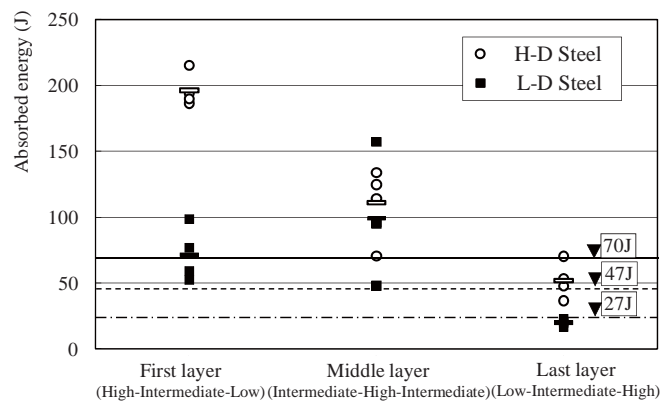


**Fig 11** Relationship between the order of achieved temperatures and the Charpy absorbed energy

## Effect of Heat Cycle in Multi-layer Welding on Charpy Absorbed Energy

the other hand, when the order was Low–Intermediate–High, which simulated the HAZ of the last layer, the Charpy absorbed energy declined significantly to about 47 J.

In the low-toughness steel, the absorbed energy exceeded 70 J when the order was Intermediate–High–Intermediate, which simulated the HAZ of the middle layer as same as the absorbed energy when the order was High–Intermediate–Low, which simulated the heat cycle of the HAZ of the first layer. On the other hand, when the order was Low–Intermediate–High, which simulated the HAZ of the last layer, the energy remained low at approximately 20 J.

Thus, it was observed that even in the case of multi-layer welding and irrespective of the toughness of steel, the absorbed energy remained low when the maximum temperature of 1350 °C is achieved in the final pass, as in the case of the weld interface in the last layer.

### 3.3 Effects of temperature after the maximum temperature is achieved

On the basis of the previous results, it is considered that the temperature cycle of the pass after being exposed to a temperature of 1350 °C, which is achieved when the

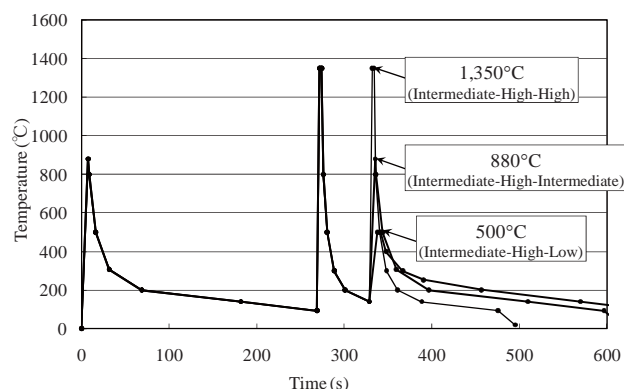


**Fig. 12** Simulated welding heat cycles (Effect of the achieved temperature after the maximum achieved temperature)

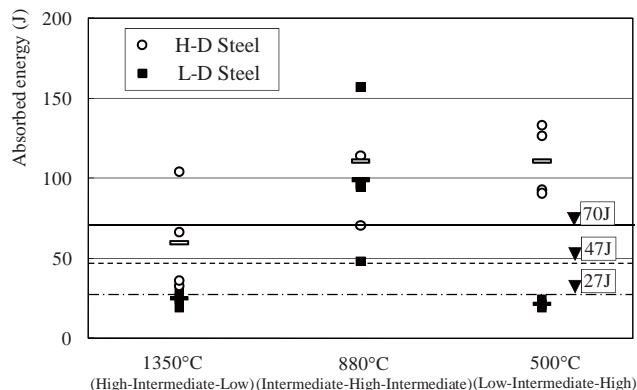


**Fig. 13** Relationship between the achieved temperature of the final pass and the Charpy absorbed energy

nearest layer is welded, significantly influences the amount of absorbed energy in the weld interface. Therefore, the authors also conducted the synthetic HAZ test with the heat cycle in which the achieved temperature of the first pass (880 °C), and that of the second pass (1350 °C) were the same, but the achieved temperature of the third pass was changed to 1350 °C (Intermediate–High–High) and 500 °C (Intermediate–High–Low). Results of Charpy impact test were compared to that with the heat cycle in which the temperature of the third pass was 880 °C (Intermediate–High–Intermediate). **Figure 12** shows the heat cycles.

**Figure 13** shows the relationship between the temperature after the maximum temperature was achieved and the Charpy absorbed energy.

In the case of the high-toughness steel, when the temperature after the maximum temperature was achieved was 1350 °C, the absorbed energy was slightly higher than 47 J, which was lower than that of the base material, as it was in the case of Low–Intermediate–High, which simulated the weld interface in the last layer. However, when the temperature after the maximum temperature was achieved was 500 °C, the absorbed energy was about 110 J, as when the temperature after the maximum temperature was achieved was 880 °C.

On the other hand, in the case of the low-toughness steel, when the temperature after the maximum temperature was achieved was 1350 °C, the absorbed energy remained low at approximately 25 J, as in the case of the Low–Intermediate–High profile, which simulated the weld interface of the last layer. When the temperature after the maximum temperature was achieved was 500 °C, the absorbed energy also remained low at approximately 20 J. Thus, it can be said that when in multi-layer welding is carried out on the low-toughness steel used in this study, the Charpy absorbed energy increases to 70 J or above only when the achieved temperature is 880 °C after the maximum achieved temperature of the weld interface of 1350 °C is reached.

As described above, in the case of the heat cycles used in this study, the Charpy absorbed energy of the weld interface was greatly influenced by the temperature after the maximum temperature was achieved. In the case of the high-toughness steel, the Charpy absorbed energy was recovered when the achieved temperature was 500–880 °C, while in the case increased only when the said temperature was approximately 880 °C.

## 4. Conclusion

The following conclusions were drawn in this study.

- (1) In the case of single-pass welding, the Charpy absorbed energy declined significantly in the weld interface of high-toughness steel. However, in the case of multi-layer welding, the Charpy absorbed energy increased more than in the case of

single-pass welding in some heat cycles, both in high-toughness steel and low-toughness steel.

- (2) On the basis of the heat cycle, it was found that when the maximum temperature of 1350 °C was reached in the final pass, the Charpy absorbed energy remained low irrespective of the steel toughness.
- (3) The Charpy absorbed energy of the weld interface was greatly susceptible to the achieved temperature after the maximum achieved temperature, and the range of the temperature after the maximum temperature was achieved in which the Charpy absorbed energy was recovered was found to be different depending on the steel toughness.

#### Acknowledgments

This study was financially supported in part by the research grant from the Japan Iron and Steel Federation. The authors would like to thank Mr. Nakatsuji and Dr. Tamagawa for their help during the experiments and the simulation.

#### References

- 1) H. KUWAMURA, H. AKIYAMA, S. YAMADA and J.-C. CHIU: Experiment on the mechanical properties and their improvement of cold press-bent steel plates, *Journal of Struct. Constr. Eng.*, (1993) No.444, pp.125-133. (in Japanese)
- 2) Y. SAKINO, S. TAKAHASHI and Y.-C. KIM: Effects of Strain Rate on Tensile Strength of Steel Specimens of HAZs with Stress Concentrations, *Quarterly Journal of the Japan Welding Society*, Vol.28 (2010) No.3, pp.328-337. (in Japanese)
- 3) Y. SAKINO, H. KAMURA and Y.-C. KIM: Charpy Absorbed Energy at CGHAZ of Rolled Steels for Building Structures Based on Simulated Heat-input, *Journal of Constructional Steel*, Vol. 13 (2005), pp.157-164. (in Japanese)
- 4) Y. SAKINO, H. KAMURA and Y.-C. KIM: Effect of Pre-Strain and Aging on Charpy Absorbed Energy in Welding Heat Affected Zone, *Journal of Structural Engineering*, Vol.52B (2006), pp.327-334. (in Japanese)
- 5) Y. SAKINO, H. KAMURA and Y.-C. KIM: Effect of Welded Condition on Charpy Absorbed Energy of Heat Affected Zones in Low Toughness Steel, *Steel Construction Engineering*, Vol.17 (2010) No.67, pp.43-52. (in Japanese)
- 6) M. MOCHIZUKI and M. TOYODA: Effects of Welding Multiple Heat Cycles on Joint Performance in Beam-to-Column Welded Connection of Steel Framed Structures — Studies on Relation between Joint Performance and Welding Heat Cycles in Welded Joints (Report 1) —, *Quarterly Journal of the Japan Welding Society*, Vol.21 (2003) No.1, pp.46-53. (in Japanese)
- 7) Y.-C. KIM, J.-Y. LEE and K. INOSE: High Accurate Prediction of Welding Distortion Generated by Fillet Welding, *Quarterly Journal of the Japan Welding Society*, Vol.23 (2005) No.3, pp.431-435. (in Japanese)
- 8) H. KUWAMURA and Y. MATSUMOTO: Fracture Resistance of 800-MPa Steel Subjected to Heat Cycles, *Journal of Struct.Constr.Engng.*, No.484 (1996), pp.101-109. (in Japanese)